Interactions between Temozolomide and Guanine and its S and Se-Substituted Analogues

Journal:	*International Journal of Quantum Chemistry*
Manuscript ID	QUA-2016-0257.R1
Wiley - Manuscript type:	Full Paper
Date Submitted by the Author:	n/a
Complete List of Authors:	Kasende, Okuma; Utah State University, Department of Chemistry & Biochemistry aris, matondo; Universite de Kinshasa, chemistry muya, jules; Universite de Kinshasa, chemistry Scheiner, Steve; Utah State University, Department of Chemistry & Biochemistry
Keywords:	dispersion, NBO, electron density shift, molecular electrostatic potential

Interactions between Temozolomide and Guanine and its S and Se-Substituted Analogues

Okuma Emile Kasende*, Aristote Matondo, Jules Tshishimbi Muya
Faculty of Science University of Kinshasa,
B.P. 190 Kinshasa XI, D. R. Congo
okuma.kasende@unikin.ac.cd

Steve Scheiner*
Department of Chemistry & Biochemistry Utah State University,
Logan, UT 84322-0300, USA
steve.scheiner@usu.edu

Abstract

Temozolomide was paired with guanine, 6-selenoguanine, and 6-thioguanine, as well as the SH tautomer of the latter. The potential energy surface of each heterodimer was searched for all minima, using Dispersion-Corrected Density Functional Theory and MP2 methods. Among the dozens of minima, three categories were observed. Stacked geometries place the aromatic systems of the two molecules parallel to one another, while the two systems are roughly perpendicular to one another in a second category. Also found are coplanar structures held together by H-bonds. Dispersion proves to be a dominating attractive force for the stacked structures, less so for perpendicular, and smallest for the coplanar dimers. Geometries and energetics are relatively insensitive to S and Se substitution, but tautomerization reverses relative stabilities of different geometries.

keywords: dispersion; NBO; electron density shift; molecular electrostatic potential

INTRODUCTION

The temozolomide (TMZ) molecule pictured in Scheme 1 is attracting growing attention by numerous research groups by virtue of its ability to serve as a DNA alkylating agent. As the most successful antiglioma drug, TMZ can add several months to the life expectancy of malignant glioma patients.[1-8] Glioblastoma, or malignant glioma (MG), is the most aggressive adult brain cancer and accounts for more than 50% of all glioma cases diagnosed.[9] Despite research efforts, the average postdiagnosis lifespan for a MG patient is 14.6 months with most patients experiencing tumor relapse and outgrowth within 7 months of initial radiation therapy.[10-12]

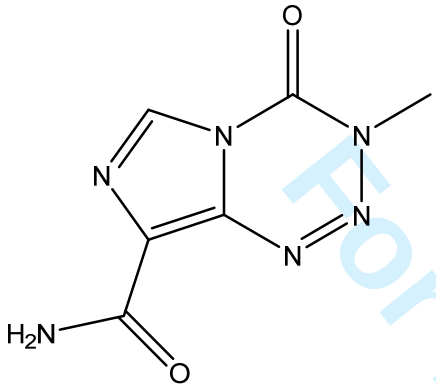

Scheme 1. Structure of temozolomide (TMZ)

From the perspective of intermolecular interactions, the chemical structure of TMZ presents a number of interesting possibilities. Its wealth of polar groups leads to the supposition that it might engage in a number of H-bonds (HBs). Its extended aromatic system presents the possibility of π-π interactions with other molecules. And the presence of a positively charged region above the ring has implications for electrostatic interactions perpendicular to the TMZ molecule. Noncovalent interactions of this sort are well known to play a ubiquitous role in numerous biological systems,[13-28] and as an added factor may serve to enhance the anticancer potency of TMZ by fostering its interaction with other pharmacologic agents.

As a means to focus on certain fundamentals, interactions of TMZ with small molecules has been examined previously by this laboratory, specifically H_2O, HCl, BH_3, and BF_3.[29-31] Using the lessons learned, work progressed to larger pharmacological agents chloroquine and quercetin, as well possible homodimers of TMZ.[32-34] Progressing toward other aspects of biological activity, the interaction of TMZ with each of the nucleic acid bases was examined and demonstrated the possibility of binding much like the standard Watson-Crick pairing that is instrumental to the structure and function of DNA.[35] But at the same time, quite different sorts of geometries, energetically similar to or even more stable than such pairing were revealed for the first time.

We turn in the current communication to variants of the nucleic acid bases. The replacement of the carbonyl O atom of guanine with larger chalcogen atoms S and Se ought to allow refinements of some of the earlier ideas. Earlier work has already confirmed that the molecular parameters of 6-thioguanine (6TG) and 6-selenoguanine (6SeG) are similar to those of native guanine (G),[36] which suggests the possibility of replacing G by its heavier analogs in nucleotides, which could rationalize the observed biological activity of these species. Even so, this substitution may induce changes in the properties of the nucleobases, which may affect, in turn, the recognition by proteins or other nucleobases, as well as the ability to stabilize the DNA double helix.

Whereas these substitutions of the carbonyl oxygen are fairly conservative, they present a number of interesting questions. How might G and its isosteres 6TG and 6SeG interact with TMZ and how will the substitutions affect the binding strength? Will the preferred geometry of the G/TMZ dimer be conserved after these substitutions? Are there certain steric clashes related to heteroatom sizes which may influence the dimer structure? Does the substitution change the nature of the forces that produce the attractive force? For instance, does dispersion play a larger role for one substituent than for another, or do electrostatic attractions die down as the chalcogen atom becomes larger?

To this point, neither experimental nor theoretical work has examined the interaction between TMZ, or related molecule, and these guanine analogues. In fact, despite of the fact that great interest has recently arisen in the nature of unconventional HBs[37-40] only a few thorough theoretical works are available where HBs involving selenium atoms have been considered.[41,42] The present study is designed to provide answers to some of these questions via quantum chemical calculations that can focus on the fundamentals of the intermolecular forces. The intermolecular recognition issues between the isosteres of G and TMZ prodrug are examined. The full range of possible dimer geometries is calculated, and their relative energies and modes of binding elucidated.

It is worthwhile mentioning parenthetically that these particular G analogs are of current biological interest. The 6TG molecule is a known metabolic inhibitor with antineoplastic activity, and is used in cancer treatment and research.[43-46] Seleno-derivatives of nucleobases have been less investigated than the corresponding thio analogues, but the available data suggest that 6SeG represents an active drug against lymphomas[47,48] and hepatomas.[49,50]

COMPUTATIONAL METHODS

Guanine N_9H amino-ketone (G) displayed in Scheme 2 was examined along with three of its derivatives. This particular tautomer of G is not the global minimum (which is the N_7H conformer), but was chosen for study here because it represents the form that is present within DNA. Replacement of the carbonyl O of G leads to its SG derivative in Scheme 2. Tautomerism of SG investigated by IR spectra in an argon matrix shows that it occurs mainly in the SGH form [51,52] with a pendant SH group, in agreement with *ab initio* calculations.[53] With regard to the position of the other NH proton, X-ray analysis[54] and other IR and Raman solid state studies[55] demonstrate that SG exists as the N_7H amino-thione tautomer in the crystal structure[54]; this is in sharp contrast with G in the crystal and in solution.[55-57] Such differences between theoretical predictions of relative stabilities and the structure experimentally observed in the crystal may be a result of the intermolecular interactions, particularly H-bonding in the crystal which are not considered in the calculations. As in the case of guanine, the N_9H form is examined here due to its similarity to the form of G observed within the confines of DNA.

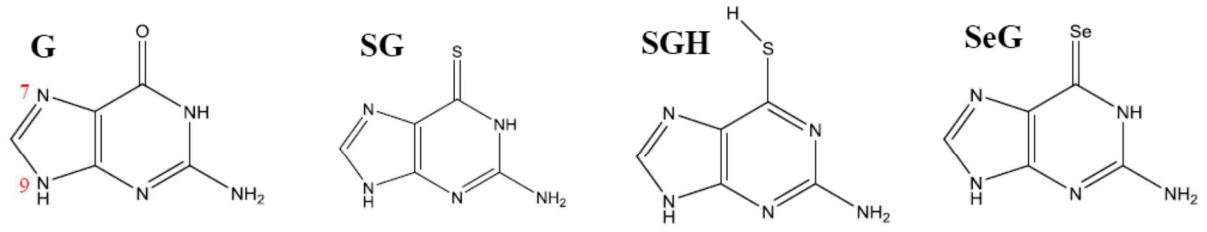

Scheme 2. Structures of guanine and several of its derivatives

With regard to the Se analogue, previous high level *ab initio* calculations revealed that the N_7 protonated form is most stable in the gas phase, 13 kJ·mol^{-1} more stable than N_9H SeG at the MP2/6-311++ G(d,p)//MP2/6-31G(d,p) level.[58] However, aqueous solvation studies using the SCI-PCM continuum models show a different trend. Free energies of tautomerization in an aqueous medium indicate that N_9H SeG is more stable than the N_7 protonated form although by only a slim margin.[58]

The geometries of heterodimers pairing each of the systems in Scheme 2 with TMZ complexes fully optimized using the M06-2X/6-31+G(d,p) protocol. Vibrational analysis verified each structure as a true minimum. Single point calculations of these heterodimers were carried out at the B3LYP, B3LYP-D3, M06-2X, ωB97XD and MP2 levels with the same basis set.[59-68] Checks for basis set consistency were performed by evaluating energies with the larger cc-pVTZ basis set, with the M06-2X functional. As the potential energy surface of each heterodimer likely contains a number of minima, a range of different starting points were taken for each geometry optimization, so as to avoid omitting any such minima. A large number (100) of different starting points were considered for each with all reasonable intermolecular configurations considered, including parallel, perpendicular, coplanar, and various mixed geometries. The final group of non-repeating, fully optimized minima comprised some 10-12 different structures for each pair, as described below. The binding energy BE of each TMZ dimer was computed as the energy difference between the optimized dimer and the sum of the relaxed monomers in their optimized geometries. This BE was corrected for basis set superposition error (BSSE)[69] using the Boys-Bernardi counterpoise correction.[70]

The dispersion energy (Disp) was estimated as the difference in BE between B3LYP-D3 and B3LYP data as described by Equation (1). The molecular electronic energies E were computed by dispersion-corrected DFT given by Equation (2), in which E_{DFT} is the (all-electron) KS-DFT SCF energy for a particular density functional, $E^{(2)}_{disp}$ is the standard atom pair-wise London dispersion energy from D3 theory[71] (using Becke-Johnson damping),[72-74] and $E^{(3)}_{disp}$ is a three-body dispersion term (of Axilrod-Teller-Mutto type),[75,76] which was calculated as described in reference [71] using program DFT-D3.[77]

$$Disp = BE_{(B3LYP\text{-}D3)} - BE_{(B3LYP)} \quad (1)$$

$$E = E_{DFT} + E^{(2)}_{disp} + E^{(3)}_{disp} \quad (2)$$

Calculations were performed using the Gaussian 09 software package.[78] Atomic charges and charge transfer energies were assessed by NBO 6.0 software.[79] GaussView and Chemcraft programs were used for visualization.[80] The molecular electrostatic potential (MEP) was evaluated for each of the monomers in their optimized geometry at the M06-2X/6-31+G(d,p) level. Electron density shifts caused by complexation were visualized as the difference between the electron density of the complex and the sum of those of the monomers, again in the geometry within the complex.

RESULTS

Geometries and Energetics

The optimized structures of all of the heterodimers with TMZ fall into one of three categories. Stacked (S) geometries where the TMZ molecule lies above and approximately parallel to the other monomer facilitate interactions between the π systems of the two. HB interactions are clearly the dominant attractive force in the HB geometries in which the two molecules are approximately coplanar. The planes of the two

molecules are roughly perpendicular (P) to one another in a sort of T-shape. Figures 1-3 depict respectively the stacked, coplanar and perpendicular arrangements of lowest energies along with the atom-numbering scheme of each pair. The remaining dimers are displayed in the SI. Some of the most important characteristics of the various minima are respectively listed in Tables 1-4. The minima are ordered by their stability at the M06-2X level, but this order can differ with some of the other levels considered here. Also reported in these tables are the NBO charge transfer energies E(2) that exceed a criterion of 2 kJ/mol.

Inspection of the tables reveals a certain level of ambiguity concerning the identity of the global minimum in several cases. Taking the G dimers in Table 1 as an example, G1 and G2 are very close in energy for all levels, with the exception of MP2 which places stacked G1 lower in energy than perpendicular G2 by some 4 kJ/mol. In contrast to the other levels, both ωB97-XD and B3LYP-D3 point to coplanar G3 as global minimum. It may be noted that G3 is stabilized by two very strong NH··O HBs, both shorter than 1.9 Å, and with E(2) in excess of 85 kJ/mol. G1 and G2 both contain one or more NH··O HBs but these are considerably weaker, with E(2) ~ 30 kJ/mol.

Replacement of the guanine carbonyl O by S leads to a clearer picture in terms of relative stabilities. Stacked structure SG1 is unanimous choice for most stable by a compelling margin for M06-2X and MP2. ωB97-XD and B3LYP-D3, on the other hand, place coplanar SG2 within only 2-3 kJ/mol of SG1, a trend which reinforces the predilection of these two functionals to favor such coplanar geometries seen with G. Note that in the SG case, perpendicular structures are disfavored, appearing first in SG7, quite a bit higher than the global minimum.

The situation changes dramatically when the NH proton of SG is shifted onto the S atom, forming the SGH tautomer. Upon this internal rearrangement, the global minimum takes on a T-shape. The SGH1 dimer is clearly preferred over all other minima, by a margin of 5-13 kJ/mol. This distinction with SG cannot be directly attributable to the participation of the S atom per se, as it lies distant from the partner TMZ molecule in either SGH1 or SG7 in Fig 3. The dominant HB in SGH1 is of NH··O type, reinforced by several weaker ones. There is ambiguity concerning the nature of the second most stable structure. M06-2X/6-31+G** and MP2 would award this distinction to stacked SGH2, whereas coplanar SGH3 is favored by ωB97-XD and B3LYP-D3, as well as M06-2X with the larger basis set, another indication of the preference of these two functionals to coplanar geometries.

Turning finally to the Se-derivatives, one again sees the preference of ωB97-XD and B3LYP-D3 for coplanar geometries. These two functionals place SeG2 as more stable than stacked SeG1 which is preferred by both M06-2X (with both basis sets) and MP2. As was the case with the S-analogue, the perpendicular type of dimer is disfavored by Se as well, not appearing until the 7th most stable structure in Table 4. In fact, this particular geometry is the only perpendicular minimum on the potential energy surface of this pair.

Comparison of individual geometries of a given type provide some insights into how substitution and tautomerization affect the binding. The four most stable stacked geometries in Fig 1, for example, show remarkable similarity between G1, SG1, and SeG1 in terms of both overall structure and H-bonding pattern. All three of them contain a pair of NH··O HBs to the carbonyl O of TMZ, as well as a weaker CH··O HB on the other end of the dimer. Indeed, the binding energies are all rather similar as well. The replacement of the O of guanine by S or Se enhances the binding energy by some 4 kJ/mol, roughly 5%. The tautomerization of SG to SGH, on the other hand considerably weakens the intermolecular binding in

SGH2, reducing it by some 30 kJ/mol. Further, there is only a single NH··O HB, and the CH··N of the other three stacked geometries is replaced by a much longer and weaker CH··S.

There is a similar sort of consistency amongst the most stable HB geometries in Fig 2. G3, SG2, and SeG2 all show the carbonyl O of TMZ engaged in a bifurcated HB with two NH groups of guanine and its analogues, with one HB much shorter than the other. One also might notice a NH··Y HB, where Y=O, S, and Se. This HB undergoes significant lengthening as the Y atom enlarges, varying from 1.876 Å for O up to 2.525 Å for Se. Along this same sequence the third HB of the system, of NH··O type, becomes shorter by 0.3 Å. These three coplanar geometries are all bound by a similar amount, between 80 and 84 kJ/mol. The SGH tautomer is again the outlier, with a much weaker interaction, and a very different HB pattern. The latter consists of a NH··O and slightly longer NH··N HB.

The consistency between G, SG, and SeG is lost in the context of perpendicular structures in Fig 3. G2 contains a network of three NH··X HBs, all between 2.0 and 2.3 Å. Upon replacement of the O of guanine by S or Se, the latter molecule flips around placing the S/Se away from TMZ rather than toward it as in G2. Three HBs remain, but the overall binding of G2 has slipped by some 23 kJ/mol in SG7 and SeG7. The orientation of the guanine derivative in SGH1 is quite similar to that in the latter two structures, as is its H-bonding pattern, but the binding energy is somewhat stronger.

Other Tautomers

SG and SGH are tautomers of one another, with comparable energies. Our calculations place the former lower in energy than the latter by 4.6 kJ/mol at the M06-2X/6-31+G** level, reduced to only 1.1 kJ/mol when the basis set is enlarged to aug-cc-pVTZ (and the geometry reoptimized), or 0.9 kJ/mol with the cc-pVTZ set. But it must be understood that the greater stability of SG does not automatically guarantee that its heterodimers with TMZ must be accordingly lower in energy than the complexes involving SGH. The italicized numbers in parentheses in Table 3 refer to the absolute energy of each of these SGHn dimers to that of the most stable SG1 complex. For example, at the M06-2X/6-31+G** level, SG1 is more stable than SGH1 by 26.39 kJ/mol. In other words, the strength of the binding in SG1 (95.4 kJ/mol) as compared to only 72.8 kJ/mol in SGH1 adds to the intrinsically lower energy of SG. It might be noted as well that the preference for SG1 over SGH1 and in fact any SGH dimers with TMZ, persists at other levels of theory as well.

As noted above the tautomer of guanine examined here is the canonical form, that occurs in nucleic acids. However, this geometry is not necessarily the lowest energy tautomer of unassociated guanine. Indeed, our calculations place the form where the proton lies on N_7 rather than N_9 as the global minimum, 9 kJ/mol lower in energy than the canonical tautomer. This situation brings up the question as to whether the dimers of this lower energy tautomer with TMZ are similarly more stable than those involving canonical guanine. This question can be answered by perusal of the values reported in parentheses in Table 1 which list the energy of the indicated heterodimer with respect to the most stable complex between TMZ and the N_7H tautomer of guanine, reported earlier.[35] It is immediately clear from some of the negative values that despite its higher intrinsic energy, the canonical N_9H tautomer forms heterodimers that are more stable than even the lowest energy dimer of N_7H guanine. Note that this reversal is true not only of the most stable G1 dimer, but of G2 and G3 as well, and extends over a full range of levels of theory. This stability reversal can be attributed to the stronger interactions of N_9H guanine with TMZ. Taking the M06-2X/6-31+G** data as illustrative, the binding energy of the G1 dimer exceeds that of the comparable dimer of the N_7H tautomer by some 9 kJ/mol.

Another interesting facet concerns the type of structure represented by the most stable dimer with TMZ of each tautomer of guanine. In the N_9H case considered here, there is a close competition between stacked, perpendicular, and coplanar structures for this distinction, depending upon level of theory. There is some uncertainty in the N_7H case as well, but the two candidates comprise perpendicular and coplanar structures, with the best stacked geometry clearly less stable. Focusing on the superior binding of the N_9H tautomer, a comparison of the perpendicular geometries, topologically quite similar with the same H-bonding pattern, shows shorter NH··O HBs as compared to N_7H: 1.994 and 2.258 Å, as compared to 2.005 and 2.411 Å for N_7H.

Influence of Dispersion

As explained above and as has been applied previously, one can assess the dispersion energy by direct comparison of B3LYP-D3 where dispersion is explicitly included with B3LYP where it is not. The binding energies by B3LYP-D3 and B3LYP methods are displayed in Tables 5-8 for the complexes of TMZ with guanine and each of its derivatives. The third column of each table contains their difference, which may be taken as a reasonable approximation of the dispersion energy.

A clear pattern emerges from inspection of the data in these tables. Taking the guanine data in Table 5 as an example, the stacked (S) structures contain the largest amount of dispersion, varying between 49 and 70 kJ/mol. There is a smaller amount of dispersion in the perpendicular dimers, 24-36 kJ/mol, but the coplanar (HB) configurations have the smallest such contribution less than 17 kJ/mol. This order makes sense from the perspective of contact between the molecules, and is consistent with observations in analogous dimers.

In terms of comparisons between O, S, and Se, one can look first at the most stable stacked dimer of each derivative. The dispersion energy for G is 49 kJ/mol, which rises to 58 kJ/mol for SG, and then up to 63 kJ/mol for the Se-derivative. A similar O < S < Se trened is apparent as well in the set of HB and P dimers.

Electrostatic Potentials

As two molecules approach one another, their medium range interactions will be largely dominated by Coulombic forces wherein the positive regions of one monomer will be attracted to negative areas of its partner, and vice versa. In a number of cases in the literature, the strength of the interaction has been directly related to the MEP of the molecules of interest. The MEP has been particularly useful as an indicator of the sites or regions of molecules to which an approaching electrophile is attracted,[81] and it has also been applied successfully to the study of interactions that involve a certain optimum relative orientation of the reactants, such as a drug and its cellular receptor.[82,83]

For that reason, the molecular electrostatic potentials (MEPs) of the molecules of interest are presented in Fig 4, where dark blue regions indicate the most positive regions, while the extreme negative areas are indicated in red. Guanine and its thio and seleno derivatives SG and SeG all display a generally similar pattern, represented by blue positive potential around the various NH groups. Negative red sections are located around unprotonated N atoms, as well as the O/S/Se atoms. The corresponding MEP around TMZ was previous reported.[29-35] This MEP in Fig 4 exhibits primary negative potential around its two O atoms, with positive regions around its H atoms and directly above its six-membered ring.

The lack of sensitivity of the MEPs of guanine and its derivatives to substitution of O by S or Se helps explain the similarities noted in the sorts of dimers formed and in their interaction energies with TMZ. The dispersal of the negative region around the S atom in the SGH tautomer is consonant with the SGH3 dimer

geometry in Fig 2 wherein the S atom is turned away from the TMZ and plays no role in HB formation. The positive region above the six-membered ring of TMZ helps account for the perpendicular dimers in Fig 3 where a negative region of the guanine derivative lies directly above this ring. Further, the lack of a positive region above either ring in G or any of its derivatives is consistent with the failure of any dimers to appear on the potential energy surface wherein a negative area of TMZ lies above a guanine ring in any sort of perpendicular structure.

Electron Density Shifts

The manner in which the electron density of each monomer adjusts to the presence of its partner is capable of providing additional insights into the fundamental binding. The electron density shift (EDS) maps in Fig 5 were constructed by subtracting the sum of the densities of the two unperturbed monomers from that of the density of the entire dimer. The purple regions represent gains of density and losses are indicated by green. The dimers were chosen to represent each of the three categories of geometry observed here as well as to illustrate the density shifts associated with S and Se substituents.

First considering a coplanar H-bonded structure, TGS2, the three HBs are reflected by the green loss around the bridging protons and the purple gain in the vicinity of the proton-acceptor atoms, typical of HBs of all sorts. The maps of the coplanar O and Se analogues of TSG2 are quite similar to one another. The NH··O HBs of the stacked guanine/TMZ global minimum G1 are likewise marked by the similar green/purple fingerprint of such bonds. In addition, there are regions of loss and gain above and below the aromatic systems of the two monomers that are reflective of inductive charge transfers that are such an important element of the binding in these stacked structures. Indeed, the pattern is barely changed upon replacing the O atom of guanine by Se, as evident by comparison with the SeG1 diagram in Fig 5. The SGH1 dimer is representative of perpendicular geometries. As shown in Fig 5, the density shifts are consistent with the HB patterns that emerge from the NBO analysis, peppered by a small amount of redistribution within the TMZ aromatic system.

SUMMARY AND DISCUSSION

Temozolomide interacts with each of guanine, 6-thioguanine, and 6-selenoguanine to form a large number of stable dimers. Some of these complexes are roughly equal in energy so that the identification of the global minimum is not entirely clear. In general, the most stable dimers place the aromatic systems roughly parallel to one another in a stacked arrangement. Dispersive forces constitute a large fraction of the binding energy of these dimers. Replacement of O by S and Se progressively increases the dispersion energy of these stacked structures, although the total binding energy is fairly insensitive to such substitution. A second common motif is a coplanar arrangement of the two molecules, held together almost exclusively by HBs. S and Se substitution has little effect upon the binding energies of guanine with TMZ for these coplanar structures as well. The molecules approach one another in a perpendicular arrangement as a third type of geometry. While this structure is quite stable for guanine, it represents a much higher energy dimer for S and Se-substituted analogues. On the other hand, the perpendicular structure of the SH tautomer of thioguanine is its likely global minimum, more stable than either stacked or coplanar structures.

Earlier work has addressed issues dealing with relative stabilities of various tautomers of guanine monomer and some of its derivatives. A prior study [36] considered guanine (Y=O) and its S and Se-substituted variants. In all cases, the N_7H tautomer was found preferable to N_9H, more so for S and Se than for O. With respect to the possible protonation of this Y atom, this sort of geometry was favored by a very

thin margin for Y=S, but disfavored for both O and Se. These conclusions differed with a thorough examination of numerous tautomers of thioguanine the following year[84] that concluded that the N_9H tautomer, the one considered in this work, is preferred. Application of large basis sets at 4th order MP theory [85] later suggested the relative stability of these two tautomers of thioguanine is a sensitive issue, which can be reversed through consideration of zero-point vibrational energies, or by inclusion of solvation effects. The same is true regarding SG and SGH, i.e. whether the S atom is or is not protonated.

The results provided here document the relative strengths of H-bonding and π-π stacking. While the former controls the coplanar structures, and the stacked geometries are dominated by the latter, there is also present a third type of geometry. The perpendicular structures combine the strengthening effect of HBs, albeit weakened by certain geometrical distortions, with the dispersion attractions that arise from the close contact of the two monomers. One sees a delicate balance between these various forces, a balance which can be shifted by certain small substitutions, and tautomeric equilibria.

The results can be placed in a broader context. As mentioned earlier, TMZ serves as a prototype of molecules that contain both an aromatic system and a set of polar atoms and groups as well. While the former tends toward π-π interactions, the latter have a natural predilection to engage in HBs. H_2O and HCl, for example, lie exclusively in the plane of the TMZ molecule, and the primary binding mode[29,31] involves HBs to O and N atoms of TMZ. While also situated in the TMZ plane, Lewis acids BH_3 and BF_3, engage in direct bonding[30] between B and the O or N atoms of TMZ, also avoiding the region above the aromatic system.

The situation changes quite dramatically when the partner molecule acquires an aromatic system of its own. When paired with chloroquine[33] π-stacking becomes a stronger orienting force than the HBs that are possible with TMZ. On the other hand, the stable geometries of the chloroquine/TMZ heterodimer permit a small number of HBs to act as a supplement to the π-π stacking force. In the case of the homodimer of TMZ [32] it is difficult for both π-stacking and HBs to coexist. It is in fact the π-π forces which are the more important, making the stacked dimers preferable to coplanar H-bonded geometries, despite the presence of two very strong NH••O HBs in the latter.

The importance of π-π stacking has been recognized for some time [86-92]. As a recent example, an examination of such forces [89] included a variety of nucleobases combined with acenapthalene and phenalenyl radical that both contain extended aromatic systems. Geometries adopted were of the stacked variety, forgoing any HBs that might otherwise be formed with the latter π-systems. These forces are apparent also in larger systems, such as the interaction of benzene with fullerene,[93] dominating other geometries that contain HBs. And as recognized in earlier work, it is dispersion that acts as the prominent component in these interactions. Even in the absence of an aromatic system as such, π-π attractions can serve as a strong driving force. This point is perhaps most evident [94] in the simple case of a pair of amides, wherein the stacked dimer is nearly as stable as that in the classic structure where strong HBs are present. This same concept accounts also for geometries adopted by γ-tripeptides and some related systems [95-97].

ACKNOWLEDGMENTS

O.E.K. would like to thank the Council for International Exchange of Scholars (CIES) for a Fulbright Visiting Scholar grant at Utah State University. Computer, storage and other resources from the Division of Research Computing in the Office of Research and Graduate Studies at Utah State University are gratefully acknowledged.

REFERENCES

[1] E.S. Newlands, M.F. Stevens, S.R. Wedge, R.T. Wheelhouse, C. Brock, *Cancer Treat. Rev.* **1997**, *23*, 35.
[2] M.J.M. Darkes, G.L. Plosker, B. Jarvis, *Am. J. Cancer*, **2002** *1*, 55.
[3] S.M. Hassani1, S. Bagheri, H. Ghahremani, *Ann. Biol. Res.* **2012**, *3*, 2393.
[4] K.M. Hvizdos, K.L. Goa, *CNS Drugs,* **1999,** *12*, 237.
[5] B.J. Denny, R.T. Wheelhouse, M.F. Stevens et al. *Biochemistry* **1994,** *33*, 9045.
[6] M.F. Stevens, J.A. Hickman, S.P. Langdon, D. Chubb, L.Vickers, R. Stone, G. Baig, C. Goddard, N.W. Gibson, J.A. Slack et al. *Cancer Res*.**1987**, *47*, 5846.
[7] H.S. Friedman, T. Kerby, H. Calvert, *Clin. Cancer Res*. **2000,** *6*, 2285.
[8] I.M. Ghobrial, T.E. Witzig, A. Adjei *C.A. Cancer J. Clin.* **2005**, *5*,178.
[9] Central Brain Tumor Registry of the United States (CBTRUS) *Report* **2010** http://www.cbtrus.org/factsheet/factsheet.html.
[10] R. Stupp, W.P. Mason, M.J. Van Den Bent et al. *N. Eng. J. Med.* **2005**, *352*, 987.
[11] L.M. DeAngelis *N. Eng. J. Med.* **2001**, *344*, 114.
[12] E.R. Laws, I.F. Parney, W. Huang et al. *J. Neurosurg.* **2003**, *99*, 467.
[13] P. Hobza, K. Müller-Dethlefs, Non-covalent interactions: theory and experiment. Royal Society of Chemistry, Cambridge UK, **2010.**
[14] A. Karshikoff, Non-covalent interactions in proteins. World Scientific, London, **2006.**
[15] S. Scheiner, Noncovalent forces. Springer, Switzerland, **2015**.
[16] A.M. Maharramov, K.T. Mahmudov, M.N. Kopylovich, A.J.L. Pombeiro, Non-covalent interactions in the synthesis and design of new compounds. Wiley, New York, **2016**.
[17] H. Lodish, Molecular cell biology 4th edn. Freeman, New York, **2000**.
[18] P. Schuster, G. Zundel, C. Sandorfy, The hydrogen bond, recent developments in theory and experiments. North-Holland Publishing Co, Amsterdam, **1976**.
[19] P. Schuster, Hydrogen bonds. Springer, Berlin, **1984**.
[20] G.A. Jeffrey, W. Saenger, Hydrogen bonding in biological structures. Springer, Berlin, **1991**
[21] S. Scheiner, Hydrogen bonding: A theoretical perspective. Oxford University Press, New York, **1997**.
[22] G. Gilli, P. Gilli, The nature of the hydrogen bond. Oxford University Press, Oxford, **2009**.
[23] R. Wieczorek, J.J. Dannenberg, *J. Am. Chem. Soc.* **2003**, *125*,8124.
[24] I.V. Alabugin, M. Manoharan, S. Peabody, F. Weinhold, *J. Am. Chem. Soc*. **2003**, *125*, 5973.
[25] H. Hernández-Soto, F. Weinhold, J.S. Francisco, *J. Chem. Phys.* **2007***, 127*, 164102.
[26] J.E. DelBene, I. Alkorta, J. Elguero, *Phys. Chem. Chem. Phys.* **2011**, *13*, 13951.
[27] T.S. Thakur, M.T. Kirchner, D. Blaser, R. Boese, G.R. Desiraju, *Phys. Chem. Chem. Phys.* **2011**, *13*, 14076.
[28] C.T. Lee, W. Yang, R.G. Parr, *Phys. Rev*. **1988**, *B37*, 785.
[29] O.E. Kasende, A. Matondo, M. Muzomwe, J.T. Muya, S. Scheiner, *Comput. Theor. Chem*. **2014**, *1034*, 26.
[30] O.E. Kasende, J.T. Muya, S. Scheiner, *Struct. Chem.* **2015,** *26*, 1359.
[31] O.E. Kasende, A. Matondo, J.T. Muya, S. Scheiner, *Comput. Theor. Chem*. **2016**, *1075*, 82.
[32] O.E. Kasende, J.T. Muya, V.de P. Nziko, S. Scheiner, *J. Mol. Mod.* **2016**, *22*,76.
[33] O.E. Kasende, V. de P. Nziko, S. Scheiner, *Int. J. Quant. Chem*. **2016**, *116*, 1196.

[34] O.E. Kasende, V.de P. Nziko, S. Scheiner, *Struct. Chem.* **2016** DOI 10.1007/s11224-016-0788-8
[35] O.E. Kasende, V. de P. Nziko, S. Scheiner, *J. Phys. Chem. B* **2016** (submitted)
[36] J. Leszczynski, *J. Mol. Struct. (THEOCHEM)*, **1994**, *311*, 37.
[37] I. Alkorta, J. Elguero, S.J. Grabowski, *J. Phys. Chem. A,* **2008** *112*, 2721.
[38] S.J. Grabowski, W.A. Sokalski, J. Leszczynski, *J. Phys. Chem. A*, **2005**, *109*, 4331.
[39] L. Rozas, I. Alkorta, J. Elguero, *J. Phys. Chem. A*, **1997**, *101*, 4236.
[40] F.A. Cotton, J.H. Matonic, C.A. Murillo, *J. Am. Chem. Soc.*, **1998**, 120, 6047.
[41] S.S.C. Ammal, P. Venuvanalingam, *J. Phys. Chem. A*, **2000**, 104, 10859.
[42] P. Sanz, M. Yanez, O. Mo, *J. Phys. Chem. A,* **2002**, 106, 4661.
[43] C.J. Hunter, D.F. Deen, L.J. Marton, *Int. J. Cancer*, **1989**, 44, 658.
[44] R. Pieters, D.R. Huismans, A.H. Loonen, K. Hahlen, A.J.P. Verman, *Jpn J. Cancer Res.* **1991**, *82*, 1051.
[45] M.D. Phillips, B. Nascimbeni, R.R. Tice, M.D. Shelby, *Environ Mol. Mutagen,* **1991**,*18*, 168.
[46] R. Pieters, D.R. Huismans, A.H. Loonen, G.J. Peters, K. Hahlen, A. Van der Does-van den Berg , E.R. Van Wering, A.J.P. Veerman, *Medical and Pediatric Oncology*, **1994**, 22, 299.
[47] H.G. Mautner, S-H Chu, J.J. Jaffe, A.C. Sartorelli, *J. Med. Chem.* **1963**, 6, 36.
[48] S.H. Chu, *J. Med. Chem.* **1971**, *14*, 254.
[49] L. Lin, J. Sheng, R.K. Momin, Q. Du, Z. Huang, *Nucleosides, Nucleotides, Nucleic Acids,* **2009**, *28*, 56.
[50] J. Salon, J. Jiang, J. Sheng, O.O. Gerlits, Z. Huang, *Nucleic. Acids. Res*. **2008**, *36*, 7009.
[51] O.E. Kasende, *Spectrochimica Acta A,* **2002**, *58*, 1793.
[52] K. Szczepaniak, W.B. Person, J. Leszczynski, J.S. Kwiatkowski, Adv. Biochem. **1995**, *41*, 300.
[53] C.E. Bugg, U. Thewalt, *J. Am. Chem. Soc.* **1970**, *92*, 7441.
[54] K. Singh, R.A. Yadav, J.S. Yadav, *Spectrochim. Acta* , **1991**, *47A*, 819.
[55] U. Thewald, C.E. Bugg, R. Marsh, Acta Cryst. **1971**, *B27*, 2358.
[56] M. Majoube, *J. Mol. Struct.* **1984**, *114*, 403.
[57] D. Shugar, A. Psoda In: Nucleic Acids. Landolt-. Bernstein New Series of Biophysics, Part I. Springer Verlag, Berlin, **1990.**
[58] D. Venkateswarlu, J. Leszczynski, *J. Phys. Chem. A,* **1998**, *102*, 6161.
[59] A.D. Becke, *J. Chem. Phys.* **1993**, *98*, 5648.
[60] S. Grimme, *WIREs Computational Molecular Science*, John Wiley & Sons Ltd **2011**, 211.
[61] Y. Zhao, D.G. Truhlar, *Theor. Chem. Account,* **2008**, *120*, 215.
[62] M. Walker, A.J.A. Harvey, A. Sen, C.E.H. Dessent, *J. Phys. Chem. A*, **2013**, *117*, 12590.
[63] A.J. Cohen, P. Mori-Sánchez, W. Yang, *Chemical Reviews*, **2012**, *112*, 289.
[64] E.G. Hohenstein, S.T. Chill, C.D. Sherrill, *J. Chem. Theor. Comput.* **2008**, *4*,1996.
[65] K.E. Riley, M. Pitoňák, P. Jurečka, P. Hobza, *Chem. Rev*. **2010**, *110,* 5023.
[66] L. Ferrighi, Y. Pan, H. Grönbeck, B. Hammer, *J. Phys. Chem*. **2012**, 116, 7374.
[67] J.D. Chai, M. Head, *Phys. Chem. Chem. Phys*. **2008**, *10*, 6615.
[68] G.A. DiLabio, E.R. Johnson, A. Otero-de-la-Roza, *Phys. Chem. Chem. Phys*. **2013**, *15*, 12821.
[69] M. Gutowski, J.G.C.M. van Duijneveldt van de Rijdt, J.H. van Lenthe, F.B. van Duijneveldt *J. Chem. Phys.* **1993**, *98*, 4728.
[70] S.F. Boys, F. Bernardi, *Mol. Phys.* **1970**, *19*, 553.

[71] S. Grimme, J. Antony, S. Ehrlich, H. Krieg, *J. Chem. Phys.* **2010**, *132*, 154104.
[72] S. Grimme, S. Ehrlich, L. Goerigk, *J. Comput. Chem*. **2011**, *32*, 1456.
[73] A.D. Becke, E.R. Johnson, *J. Chem. Phys.* **2005**, *122*, 154104.
[74] E.R. Johnson, A.D. Becke, *J. Chem. Phys.* **2005**, 123, 024101.
[75] B.M. Axilrod, E Teller, *J. Chem. Phys.* **1943**, *11*, 299.
[76] J. Mutto, *Proc. Phys. Math. Soc. Japan*, **1943**, *17*, 629.
[77] S. Grimme, grimme_dftd3.3.0.2. Available at: http://www.thch.unibonn. de/
[78] M.J. Frisch, G.W. Trucks, H.B. Schlegel, G.E. Scuseria, M.A. Robb, J.R. Cheeseman, G. Scalmani, V. Barone, B. Mennucci, G.A. Petersson et al. Gaussian 09, revision A.02, Gaussian Inc., Wallingford, CT, **2009**.
[79] E.D. Glendening, J.K. Badenhoop, A.E. Reed, J.E. Carpenter, J.A. Bohmann, C.M. Morales, C.R. Landis, F. Weinhold NBO 6.0. Theoretical Chemistry Institute, University of Wisconsin, Madison, **2013**.
[80] R. Dennington, T. Keith, J. Millan, GaussView, version 5, Semichem. Inc., Shawnee Mission, KS, **2009**.
[81] O.E. Kasende, J.T. Muya, L. Broeckaert, G. Maes, P. Geerlings, *J. Phys. Chem. A,* **2012**, *116*, 8008.
[82] M. Monasterios, M. Avendano, M.I. Amaro, W. Infante, J. Charris, *J. Mol. Struct.* **2006**, *798,* 102.
[83] R.J. Xavier, P. Dinesh, *Spectrochim. Acta A*, **2014**,*118*, 999.
[84] C. Ahambra, F.J. Luque, J. Estelrich, M. Orozco, *J. Org. Chem.* **1996**, *60*, 969.
[85] M.J. Stewart, J. Leszczynski, Y.V. Rubin, Y.P. Blagoi, *J. Phys. Chem. A*, **1997**, *101*, 4753.
[86] R. K. Raju, J. W. G. Bloom, Y. An, S. E. Wheeler, *ChemPhysChem.* **2011**, 12, 3116.
[87] S. Kumar, A. Mukherjee, A. Das, *J. Phys. Chem. A* **2012**, 116, 11573.
[88] L. Yang, J. B. Brazier, T. A. Hubbard, D. M. Rogers, S. L. Cockroft, *Angew. Chem. Int. Ed.* **2016**, 55, 912.
[89] C. Trujillo, G. Sánchez-Sanz, *ChemPhysChem.* **2016**, 17, 395.
[90] J. A. Frey, C. Holzer, W. Klopper, S. Leutwyler, *Chem. Rev.* **2016**, 116, 5614.
[91] J. B. Pawliszyn, M. M. Szczesniak, S. Scheiner, *J. Phys. Chem.* **1984**, 88, 1726.
[92] T. Kar, H. F. Bettinger, S. Scheiner, A. K. Roy, *J. Phys. Chem. C* **2008**, 112, 20070.
[93] M.-M. Li, Y.-B. Wang, Y. Zhang, W. Wang, *J. Phys. Chem. A* **2016**, 120, 5766.
[94] U. Adhikari, S. Scheiner, *J. Phys. Chem. A* **2013**, 117, 489.
[95] W. H. James, E. G. Buchanan, C. W. Muller, J. C. Dean, D. Kosenkov, L. V. Slipchenko, L. Guo, A. G. Reidenbach, S. H. Gellman, T. S. Zwier, *J. Phys. Chem. A* **2011**, 115, 13783.
96] W. H. James, E. G. Buchanan, L. Guo, S. H. Gellman, T. S. Zwier, *J. Phys. Chem. A* **2011**, 115, 11960.
[97] W. H. James, C. W. Muller, E. G. Buchanan, M. G. D. Nix, L. Guo, L. Roskop, M. S. Gordon, L. V. Slipchenko, S. H. Gellman, T. S. Zwier, *J. Am. Chem. Soc.* **2009**, 131, 14243.

Table 1. Binding energies BE, and NBO second-order perturbation energy E(2) (kJ/mol) of G-TMZ dimers. *S*, *HB* and *P* designations refer to category of structure, see text. Values in parentheses refer to the energy of the indicated dimer relative to the most stable heterodimer of TMZ with the global minimum N_7H tautomer of guanine.

Dimer	BE ($kJ.mol^{-1}$)					TMZ…G	NBO E(2)
	MO62X/ cc-pVTZ	MO62X/6 -31+G**	ωB97XD/ 6-31+G**	B3LYP-D3/6-31+G**	MP2/6-31+G**		
G1 *S*	-84.12	-90.77 *(-6.51)*	-86.44 *(-5.60)*	-85.82 *(-4.54)*	-73.82 *(-7.75)*	O_{14}(LPS)→ N_{33}-H_{35}(σ*) O_{14}(LPS)→ N_{29}-H_{30}(σ*) C_1-C_9(π*)←C_{27}-O_{28}(π) N_4-N_5(π*) ← N_{29}-C_{31}(π) C_{11}-O_{14}(π) →N_{29}-H_{30}(σ*) C_8-H_{17}(π*) ← N_{26}(LP)	30.59 6.90 4.69 4.10 2.93 2.51
G2 *P*	-84.11	-90.65 *(-6.39)*	-85.02 *(-4.17)*	-84.89 *(-3.60)*	-69.62 *(-3.55)*	O_{14}(LPs)→ N_{33}-H_{35}(σ*) O_{14}(LPs)→ N_{29}-H_{30}(σ*) N_5(LP)→ N_{29}-H_{30}(σ*) C_{11}-O_{14}(π) →N_{33}-H_{35}(σ*) C_1-C_9(π*)← O_{28}(LPs) N_4-N_5(π)→ N_{29}-H_{30}(σ*) C_{11}-O_{14}(π) →N_{29}-H_{30}(σ*) C_2-O_7(π*)← O_{28}(LPs)	31.17 17.57 10.25 5.52 5.31 2.80 2.43 2.38
G3 *HB*	-81.10	-84.72 *(-0.46)*	-88.57 *(-7.73)*	-88.21 *(-6.93)*	-65.54 *(0.54)*	O_{14}(LPs)→ N_{29}-H_{30}(σ*) N_{13}-H_{18}(σ*)← O_{28}(LPs) O_{14}(LPs)→ N_{33}-H_{35}(σ*)	132.38 85.56 5.40
G4 *S*	-73.10	-80.16 *(4.10)*	-71.08 *(9.76)*	-63.64 (17.65)	-59.41 *(6.67)*	O_{14}(LPs)→ N_{33}-H_{36}(σ*) C_{11}-O_{14}(π) →N_{33}-H_{36}(σ*) C_2-O_7(π*)←C_{21}-N_{26}(π) C_1-C_9(π*)←C_{24}-C_{25}(π) C_1-C_9(π*)→C_{24}-C_{25}(π) N_4-N_5(π) → C_{27}-O_{28}(π*) C_8-H_{16}(σ*) ← N_{26}(LP) N_5(LP)→ C_{31}-N_{32}(π*)	12.84 6.74 3.93 3.22 3.14 2.97 2.80 2.55
G5 *P*	-62.79	-68.65 *(15.61)*	-67.04 *(13.80)*	-66.05 *(15.23)*	-50.98 *(15.09)*	O_{14}(LPs)→ N_{33}-H_{35}(σ*) N_4(LP)→ N_{29}-H_{30}(σ*) C_8-H_{15}(σ*)← O_{28}(LPs) N_5(LP)→ N_{33}-H_{35}(σ*) N_5(LP)→ N_{29}-H_{30}(σ*)	21.30 16.40 16.11 13.60 3.22
G6 *P*	-62.53	-68.04 *(16.22)*	-66.25 *(14.59)*	-62.94 *(18.34)*	-54.31 *(11.77)*	O_{14}(LPs)→ N_{22}-H_{23}(σ*) C_2-O_7(π*)→ N_{33}-H_{36}(σ*) N_5(LP)→ N_{22}-H_{23}(σ*) O_7(LPs)→ N_{33}-H_{36}(σ*) C_{11}-O_{14}(π) →N_{22}-H_{23}(σ*) C_8-H_{17}(σ*)← N_{33}(LP) C_2-O_7(π*)← N_{32}(LP) C_1-C_9(π*)← N_{32}(LP)	40.17 15.31 6.74 5.82 5.52 4.90 4.30 3.26
G7 *S*	-56.48	-63.05 (21.21)	-57.93 *(22.92)*	-51.77 *(29.52)*	-50.49 *(15.58)*	O_{14}(LPs)→ N_{22}-H_{23}(σ*) C_8-H_{17}(σ*)← O_{28}(LPs) C_{11}-O_{14}(π) →N_{22}-H_{23}(σ*)	9.67 5.65 5.56

						$N_3(LP) \rightarrow C_{27}\text{-}O_{28}(\pi^*)$ $C_1\text{-}C_9(\pi) \rightarrow C_{21}\text{-}N_{26}(\pi^*)$ $C_8\text{-}H_{17}(\sigma^*) \leftarrow C_{27}\text{-}O_{28}(\pi)$ $C_1\text{-}C_9(\pi) \leftarrow C_{24}\text{-}C_{25}(\pi^*)$	4.18 4.02 3.47 3.01
G8 *HB*	-54.99	-57.86 *(26.40)*	-62.51 *(18.33)*	-60.96 *(20.32)*	-46.67 *(19.41)*	$O_{14}(LPs) \rightarrow N_{22}\text{-}H_{23}(\sigma^*)$ $N_{13}\text{-}H_{18}(\sigma^*) \leftarrow N_{32}(LP)$	98.83 61.34
G9 *HB*	-51.02	-53.72 *(30.53)*	-58.94 *(21.90)*	-57.53 *(23.75)*	-34.94 *(31.14)*	$O_{14}(LPs) \rightarrow N_{33}\text{-}H_{36}(\sigma^*)$ $N_{13}\text{-}H_{18}(\sigma^*) \leftarrow N_{32}(LP)$	93.60 71.30
G10 *HB*	-46.00	-49.75 *(34.51)*	-52.91 *(27.93)*	-53.56 *(27.73)*	-33.93 *(32.14)*	$O_7(LPs) \rightarrow N_{29}\text{-}H_{30}(\sigma^*)$ $C_{10}\text{-}H_{20}(\sigma^*) \leftarrow O_{28}(LPs)$ $O_7(LPs) \rightarrow N_{33}\text{-}H_{35}(\sigma^*)$	63.64 44.64 11.38

Table 2. Binding energies BE, and NBO second-order perturbation energy E(2) (kJ/mol) of SG-TMZ dimers.

Dimer	BE (kJ.mol^{-1})					TMZ…SG	NBO E(2) (kJ.mol^{-1})
	MO62X/ cc-pVTZ	MO62X/ 6-31+G**	ωB97XD /6-31+G**	B3LYP-D3/6-31+G**	MP2/6-31+G**		
SG1 *S*	-88.07	-95.44	-90.43	-88.01	-86.74	O_{14}(LPs)→ N_{33}-H_{35}(σ*) O_{14}(LPs)→ N_{29}-H_{30}(σ*) C_{11}-O_{14}(π) →N_{29}-H_{30}(σ*) N_4-N_5(π*)← N_{29}(LP) N_4-N_5(π*)→C_{27}-S_{28}(π) C_8-H_{16}(σ*)← N_{26}(LP) C_2-O_7(π*)←C_{27} -S_{28}(LPs) C_1-C_9(π*)←C_{27}-S_{28}(π)	41.55 11.84 6.69 4.39 3.05 2.94 2.64 2.55
SG2 *HB*	-80.56	-83.92	-87.32	-86.20	-69.21	O_{14}(LPs)→ N_{29}-H_{30}(σ*) N_{13}-H_{18}(σ*)←S_{28}(LPs) O_{14}(LPs)→ N_{33}-H_{35}(σ*)	105.31 73.80 20.25
SG3 *S*	-72.17	-80.28	-74.89	-67.58	-70.60	O_{14}(LPs)→ N_{33}-H_{35}(σ*) C_1-C_9(π*)← C_{31}-N_{32}(π) C_{11}-O_{14}(π) →N_{33}-H_{35}(σ*) N_6(LP)→ N_{22}-C_{24}(π*) C_1-C_9(π*)→C_{31}-N_{32}(π)	18.74 3.81 3.26 2.68 2.22
SG4 *S*	-72.85	-79.94	-72.42	-65.31	-69.98	C_2-O_7(π*)← C_{27}-S_{28}(π) O_{14}(LPs)→ N_{33}-H_{36}(σ*) C_{11}-O_{14}(π*)← C_{31}-N_{32}(π) C_{11}-O_{14}(π) →N_{33}-H_{36}(σ*) N_5(LP)→ N_{33}-H_{35}(σ*)	4.39 3.22 3.18 2.76 2.05
SG5 *S*	-62.86	-69.83	-65.15	-56.41	-68.37	O_{14}(LPs)→ N_{22}-H_{23}(σ*) C_1-C_9(π)→ N_{22}-H_{23}(σ*) C_{11}-O_{14}(π)→ N_{22}-H_{23}(σ*) C_{10}-N_{12}(π*)←C_{27}-S_{28}(π) N_4-N_5(π)→C_{21}-N_{26}(π*) C_1-C_9(π) ← C_{21}-N_{26}(π*)	6.32 4.94 4.06 3.31 3.10 2.34
TGS6 *HB*	-65.09	-69.56	-70.48	-69.59	-56.31	N_4(LP)→ N_{29}-H_{30}(σ*) N_5(LP)→ N_{33}-H_{35}(σ*) C_8-H_{15}(σ*)←S_{28}(LPs) O_{14}(LPs)→ N_{33}-H_{35}(σ*)	35.77 34.69 23.68 9.41
SG7 *P*	-61.24	-66.63	-65.34	-62.01	-62.20	O_{14}(LPs)→ N_{22}-H_{23}(σ*) C_2-O_7(π*)→ N_{33}-H_{36}(σ*) N_5(LP)→ N_{22}-H_{23}(σ*) O_7(LPs)→ N_{33}-H_{36}(σ*) C_{11}-O_{14}(π) →N_{22}-H_{23}(σ*) C_2-O_7(π*)← N_{32}(LP) C_8-H_{16}(σ*)← N_{33}(LP) C_1-C_9(π*)← N_{32}(LP)	38.16 16.19 8.49 6.32 5.15 4.81 4.14 3.10
SG8 *S*	-54.33	-61.53	-57.14	-50.49	-54.53	C_2-O_7(π) → N_{33}-H_{36}(σ*) N_{13}-H_{19}(π*)← C_{27}-S_{28}(π) C_1-C_9(π)→ C_{24}-C_{25}(π*) C_{11}-O_{14}(π) →C_{21}-N_{26}(π*) C_{11}-O_{14}(π*) ←C_{24}-C_{25}(π)	6.61 4.06 3.10 2.93 2.89

						C_{10}-N_{12}(π)→ C_{31}-N_{32}(π*) O_7(LPs)→ N_{33}-H_{36}(σ*) N_5(LP)→ N_{22}-H_{23}(σ*)	2.55 2.47 2.26
SG9 *HB*	-45.05	-49.13	-50.62	-48.76	-44.14	N_{13}-H_{18}(σ*)← N_{26}(LP) O_{14}(LPs)→ C_{21}-H_{34}(σ*)	63.18 20.00
SG10 *HB*	-40.03	-43.89	-49.12	-46.06	-39.59	N_{12}(LP)→ N_{29}-H_{30}(σ*) N_{13}(LP)→ N_{33}-H_{35}(σ*) C_{10}-H_{20}(σ*)←S_{28}(LPs)	63.47 39.95 11.80

Table 3. Binding energies BE, and NBO second-order perturbation energy E(2) (kJ/mol) of SGH-TMZ dimers. Values in parentheses indicated energy of indicated dimer as compared to SG1.

Dimer	BE (kJ.mol^{-1})					TMZ…SGH	NBO E(2) (kJ.mol^{-1})
	MO62X/ cc-pVTZ	MO62X/ 6-31+G**	ωB97XD /6-31+G**	B3LYP-D3/6-31+G**	MP2/6-31+G**		
SGH1 *P*	-67.09	-72.83 *(26.39)*	-71.42 *(21.30)*	-67.98 *(24.02)*	-59.68 *(12.31)*	O_{14}(LPs)→ N_{22}-H_{23}(σ*) C_2-O_7(π*)→ N_{33}-H_{36}(σ*) C_8-H_{16}(σ*)← N_{33}(LP) C_{11}-O_{14}(π) →N_{22}-H_{23}(σ*) N_5(LP) → N_{22}-H_{23} (σ*) C_1-C_9(π*)← N_{32}(LP) C_2-O_7(π*)← N_{32}(LP) O_7(LPs)→ N_{33}-H_{36}(σ*)	54.48 9.29 8.62 6,82 5.15 3.68 3.43 2.38
SGH2 *S*	-54.31	-67.79 *(31.43)*	-63.09 *(29.63)*	-56.24 *(35.76)*	-55.33 *(16.66)*	O_{14}(LPs)→ N_{22}-H_{23}(σ*) C_8-H_{15}(σ*) ← S_{28}(LPs) N_4-N_5(π*)←N_{22}-C_{24}(π) C_1-C_9(π) → C_{31}-N_{32}(π*) C_{10}-N_{12}(π*)← N_{33}(LP)	65.73 6.69 3.85 2.30 2.26
SGH3 *HB*	-58.89	-61.48 *(37.75)*	-67.00 *(25.72)*	-65.26 *(26.74)*	-49.67 *(22.33)*	O_{14}(LPs)→ N_{22}-H_{23}(σ*) N_{13}-H_{18}(σ*)← N_{32}(LP)	110.54 66.23
SGH4 *S*	-52.27	-58.48 *(40.74)*	-53.95 *(38.77)*	-48.12 *(43.88)*	-44.33 *(27.66)*	N_4-N_5(π) →N_{22}-C_{24}(π*) O_{14}(LPs)→ C_{21}-H_{34}(σ*)	3.01 2.22
SGH5 *S*	-51.30	-57.26 *(41.96)*	-51.65 *(41.07)*	-45.01 *(46.99)*	-39.42 *(32.57)*	C_8-H_{16}(π*)← N_{26}(LP) C_{11}-O_{14}(π)→N_{33}-H_{35}(σ*) N_4-N_5(π) ← S_{28}(LPs) N_6(LP) →N_{22}-C_{24}(π*) C_{11}-O_{14} (π*)← N_{33}(LP)	6.28 2.89 2.76 2.55 2.26
SGH6 *P*	-51.75	-56.74 *(42.49)*	-55.84 *(36.88)*	-53.06 *(38.94)*	-40.31 *(31.68)*	C_2-O_7(π)→ N_{22}-H_{23}(σ*) O_{14}(LPs)→ N_{33}-H_{36}(σ*) O_7(LPs)→ N_{22}-H_{23}(σ*) N_5(LP) → N_{33}-H_{36} (σ*) C_2-O_7(π*)← N_{32}(LP) C_1-C_9(π*)← N_{32}(LP) C_{11}-O_{14}(π)→N_{33}-H_{36}(σ*) C_8-H_{16}(π*)← N_{22}-C_{24}(π)	16.48 14.39 13.35 5.98 3.77 3.68 3.47 2.34
SGH7 *S*	-49.64	-55.21 *(44.01)*	-49.08 *(43.64)*	-41.40 *(50.60)*	-39.26 *(32.57)*	C_1-C_9(π)→ C_{31}-N_{32} (π*) C_8-H_{16}(π*)← N_{26}(LP) C_{11}-O_{14} (π*)← N_{33}(LP) N_4-N_5(π) ←C_{21}-N_{26}(π*)	3.72 3.22 2.97 2.18
SGH8 *HB*	-44.35	-46.88 *(52.34)*	-51.05 *(41.67)*	-50.28 *(41.72)*	-28.16 *(43.84)*	N_{13}-H_{18}(σ*)← N_{29}(LP) O_{14}(LPs)→ N_{33}-H_{35}(σ*)	67.57 64.27
SGH9 *HB*	-42.61	-45.26 *(53.96)*	-50.16 *(42.56)*	-49.36 *(42.64)*	-27.87 *(44.12)*	O_{14}(LPs)→ N_{33}-H_{36}(σ*) N_{13}-H_{18}(σ*)← N_{32}(LP)	74.81 68.49
SGH10 *P*	-40.02	-44.48 *(54.75)*	-45.15 *(47.57)*	-40.54 *(51.46)*	-34.27 *(37.73)*	C_8-H_{16}(π*)← N_{33}(LP) C_2-O_7(π)→ N_{33}-H_{36}(σ*) N_{12}(LPs)→ N_{22}-H_{23}(σ*)	7.74 6.49 5.82

						C_{10}-N_{12}(π)→ N_{22}-H_{23}(σ*) N_{13}(LPs)→ N_{22}-H_{23}(σ*) O_7(LPs)→ N_{33}-H_{36}(σ*) C_1-C_9(π*)← N_{22}(LP)	4.85 3.60 2.59 2.05
SGH11 *P*	-32.77	-38.09 *(61.14)*	-39.54 *(53.18)*	-37.06 *(54.94)*	-25.92 *(46.07)*	O_{14}(LPs)→ S_{28}-H_{30}(σ*) N_{12}(LPs)→ N_{33}-H_{35}(σ*) C_{11}-O_{14}(π)→S_{28}-H_{30}(σ*) C_{10}-N_{12}(π)→ N_{33}-H_{35}(σ*) C_1-C_9(π*)← N_{92}(LP) C_{11}-O_{14}(π*)← N_{92}(LP)	29.92 20.46 9.70 5.23 3.68 2.26
SGH12 *HB*	-27.35	-32.14 *(67.09)*	-36.04 *(56.68)*	-33.75 *(58.25)*	-19.04 *(52.96)*	N_{29}(LPs)→ N_{13}-H_{19}(σ*) N_{12}(LPs)→ S_{28}-H_{30}(σ*) N_{13}(LPs)→ N_{33}-H_{35}(σ*)	51.42 31.381 10.67

Table 4. Binding energies BE, and NBO second-order perturbation energy E(2) (kJ/mol) of SeG-TMZ dimers.

Dimer	BE (kJ.mol^{-1})					TMZ…SeG	NBO E(2) (kJ.mol^{-1})
	M062X/ cc-pVTZ	MO62X/6 -31+G**	ωB97XD/ 6-31+G**	B3LYP-D3/6-31+G**	MP2/6-31+G**		
SeG1 *S*	-88.51	-95.07	-87.63	-85.31	-75.27	O_{14}(LPs)→ N_{32}-H_{34}(σ*) O_{14}(LPs)→ N_{28}-H_{29}(σ*) C_{11}-O_{14}(π) →N_{28}-H_{29}(σ*) N_4-N_5(π) ←N_{28}(LP) C_2-O_7(π*)←C_{27}-Se_{36}(π) N_4-N_5(π)→C_{27}-Se_{36}(π*) C_1-C_9(π*)←C_{27}-Se_{36}(π) C_8-H_{16}(σ*) ←N_{26}(LP)	38.49 16.19 8.49 4.56 4.35 3.60 2.93 2.80
SeG2 *HB*	-83.58	-86.79	-89.19	-88.23	-60.26	O_{14}(LPs)→ N_{28}-H_{29}(σ*) N_{13}-H_{18}(σ*)← Se_{36}(LPs) O_{14}(LPs)→ N_{32}-H_{34}(σ*)	113.97 81.88 22.09
SeG3 *S*	-72.89	-79.89	-71.58	-64.12	-56.11	O_{14}(LPs)→ N_{32}-H_{35}(σ*) C_{11}-O_{14}(π) →N_{32}-H_{35}(σ*) N_4-N_5(π*) ←C_{27}-Se_{36}(π) C_1-C_9(π) ← C_{24}-C_{25}(π*) C_1-C_9(π)→ C_{24}-C_{25}(π*) C_2-O_7(π*) ←C_{21}-N_{26}(π) N_5(LP)→ C_{30}-N_{31}(π*)	12.38 6.99 4.10 3.68 3.64 3.18 2.13
SeG4 *S*	-70.03	-77.31	-70.33	-62.69	-55.99	O_{14}(LPs)→ N_{32}-H_{34}(σ*) C_{11}-O_{14}(π) →N_{28}-H_{29}(σ*) N_6(LP)→ N_{22}-C_{24}(π *) C_1-C_9(π*)← C_{30}-N_{31}(π)	16.65 2.89 2.51 2.47
SeG5 *HB*	-67.36	-71.53	-71.37	-69.90	-45.71	N_4(LP)→ N_{28}-H_{29}(σ*) N_5(LP)→ N_{32}-H_{34}(σ*) C_8-H_{15}(σ*)← Se_{36}(LPs) O_{14}(LPs)→ N_{32}-H_{34}(σ*)	34.81 34.31 33.89 18.66
SeG6 *HB*	-66.46	-70.69	-70.11	-68.31	-46.55	N_5(LP)→ N_{32}-H_{34}(σ*) C_8-H_{15}(σ*)← Se_{36}(LPs) N_4(LP)→ N_{28}-H_{29}(σ*) O_{14}(LPs)→ N_{32}-H_{34}(σ*)	31.59 29.62 24.18 17.78
SeG7 *P*	-61.45	-67.22	-65.96	-62.47	-50.33	O_{14}(LPs)→ N_{22}-H_{23}(σ*) C_2-O_7(π)→ N_{32}-H_{35}(σ*) N_5(LP)→ N_{22}-H_{23}(σ*) O_7(LPs)→ N_{32}-H_{35}(σ*) C_{11}-O_{14}(π)→ N_{22}-H_{23}(σ*) C_2-O_7(π*) ←N_{31}(LP) C_8-H_{16}(π*) ←N_{32}(LP) C_1-C_9(σ*) ←N_{31}(LP)	41.38 16.40 7.87 6.90 5.56 4.73 4.06 3.22
SeG8 *S*	-58.67	-65.43	-58.55	-52.28	-48.52	C_8-H_{17}(σ*)← Se_{36}(LPs) O_{14}(LP)→ N_{22}-H_{23}(σ*) C_8-H_{17}(π*)← C_{27}-Se_{36}(π) N_3(LP)→ C_{27}-Se_{36}(π*) C_{11}-O_{14}(π)→ N_{22}-H_{23}(σ*) C_2-O_7(π*)← C_{27}-Se_{36}(π)	9.46 4.73 4.39 3.51 3.31 3.31

						N_4-$N_5(\pi) \rightarrow N_{22}$-$C_{24}(\pi^*)$	3.01
SeG9 *HB*	-53.08	-56.09	-61.62	-59.75	-41.47	$O_{14}(LPs) \rightarrow N_{22}$-$H_{23}(\sigma^*)$ N_{13}-$H_{18}(\sigma^*) \leftarrow N_{31}(LP)$	112.72 57.86
SeG10 *HB*	-49.00	-52.18	-57.38	-56.03	-29.91	$O_{14}(LPs) \rightarrow N_{32}$-$H_{35}(\sigma^*)$ N_{13}-$H_{18}(\sigma^*) \leftarrow N_{31}(LP)$	105.64 62.93
SeG11 *HB*	-44.39	-47.60	-50.56	-50.27	-26.43	C_{10}-$H_{20}(\sigma^*) \leftarrow Se_{36}(LPs)$ $O_7(LPs) \rightarrow N_{28}$-$H_{29}(\sigma^*)$ $O_7(LPs) \rightarrow N_{32}$-$H_{34}(\sigma^*)$	51.88 48.87 27.61

Table 5. Comparison between B3LYP and B3LYP-D3 binding energies ($kJ.mol^{-1}$) of G-TMZ dimers, all with the 6-31+G** basis set

Dimer	B3LYP-D3	B3LYP	ΔBE
G1 *S*	-85.82	-36.84	-48.98
G2 *P*	-84.89	-49.23	-35.66
G3 *HB*	-63.64	-71.90	-8.26
G4 *S*	-63.64	6.74	-70.38
G5 P	-66.05	-41.70	-24.35
G6 *P*	-62.94	-20.15	-42.79
G7 *S*	-51.77	12.45	-64.22
G8 *HB*	-60.96	-46.37	-14.59
G9 *HB*	-57.53	-43.47	-14.06
G10 *HB*	-53.56	-37.22	-16.34

Table 6. Comparison between B3LYP and B3LYP-D3 binding energies ($kJ.mol^{-1}$) of SG-TMZ dimers.

Dimer	B3LYP-D3	B3LYP	ΔBE
SG1 *S*	-88.01	-29.69	-58.32
SG2 *HB*	-86.20	-68.80	-17.40
SG3 *S*	-67.58	6.27	-73.85
SG4 *S*	-65.31	5.53	-70.84
SG5 *S*	-56.41	10.25	-66.66
SG6 *HB*	-69.59	-46.84	-22.72
SG7 *P*	-62.01	-18.91	-43.10
SG8 *S*	-50.49	19.65	-70.14
SG9 *HB*	-48.76	-35.86	-12.90
SG10 *HB*	-46.06	-22.31	-23.75

Table 7. Comparison between B3LYP and B3LYP-D3 binding energies (kJ.mol^{-1}) of SGH-TMZ dimers.

Dimer	B3LYP-D3	B3LYP	ΔBE
SGH1 *P*	-67.98	-24.75	-43.23
SGH2 *S*	-56.24	14.00	-70.24
SGH3 *HB*	-65.26	-50.75	-14.51
SGH4 *S*	-48.12	17.49	-65.61
SGH5 *S*	-45.01	27.49	-72.50
SGH6 *P*	-53.06	-10.00	-43.06
SGH7 *S*	-41.40	28.77	-70.17
SGH8 *HB*	-50.28	-32.74	-17.51
SGH9 *HB*	-49.36	-35.64	-13.72
SGH10 *P*	-40.54	4.96	-45.50
SGH11 *P*	-37.06	0.72	-37.78
SGH12 *HB*	-33.75	-12.00	-21.75

Table 8. Comparison between B3LYP and B3LYP-D3 binding energies (kJ.mol^{-1}) of SeG-TMZ dimers.

Dimer	B3LYP-D3	B3LYP	ΔBE
SeG1 *S*	-85.31	-22.72	-62.59
SeG2 *HB*	-88.23	-69.92	-18.31
SeG3 *S*	-64.12	9.93	-74.05
SeG4 *S*	-62.69	15.45	-78.14
SeG5 *HB*	-69.90	-45.89	-24.01
SeG6 *HB*	-68.31	-43.41	-24.9
SeG7 *P*	-62.47	-19.26	-43.21
SeG8 *S*	-52.28	19.39	-71.67
SeG9 *HB*	-59.75	-45.40	-14.35
SeG10 *HB*	-56.03	-42.04	-13.99
SeG11 *HB*	-50.27	-31.90	-18.37

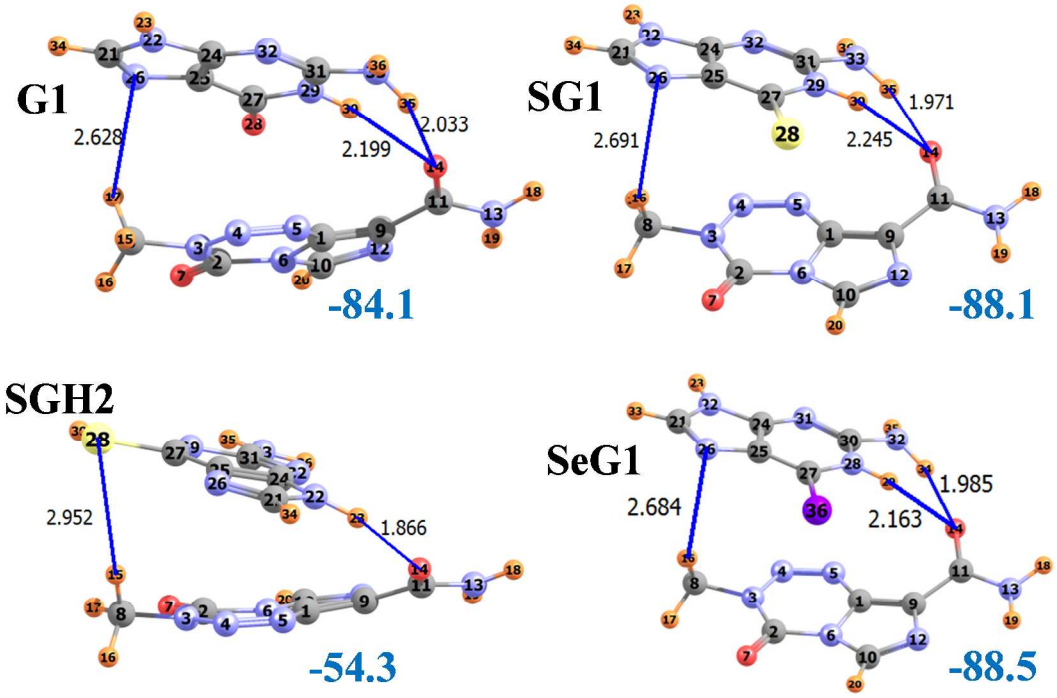

Fig 1. Geometries of the most stable stacked geometry of each guanine derivative with TMZ. Lines represent HBs indicated by NBO analysis, with distances in Å. Binding energy at M06-2X/cc-pVTZ level shown by blue number, in kJ/mol. S is yellow and Se is purple.

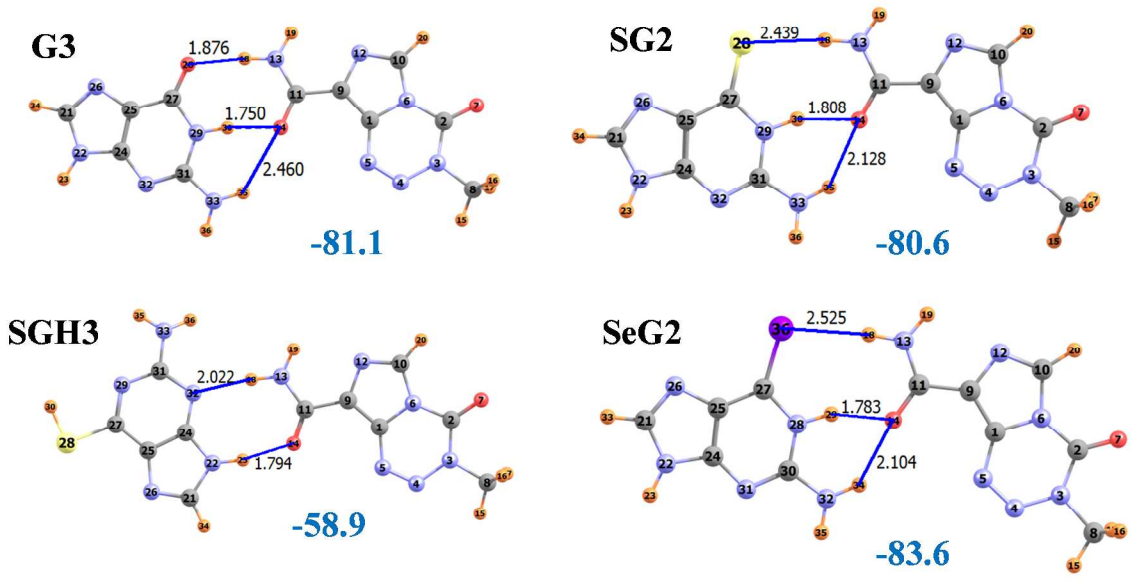

Fig 2. Geometries of the most stable coplanar geometry of each guanine derivative with TMZ.

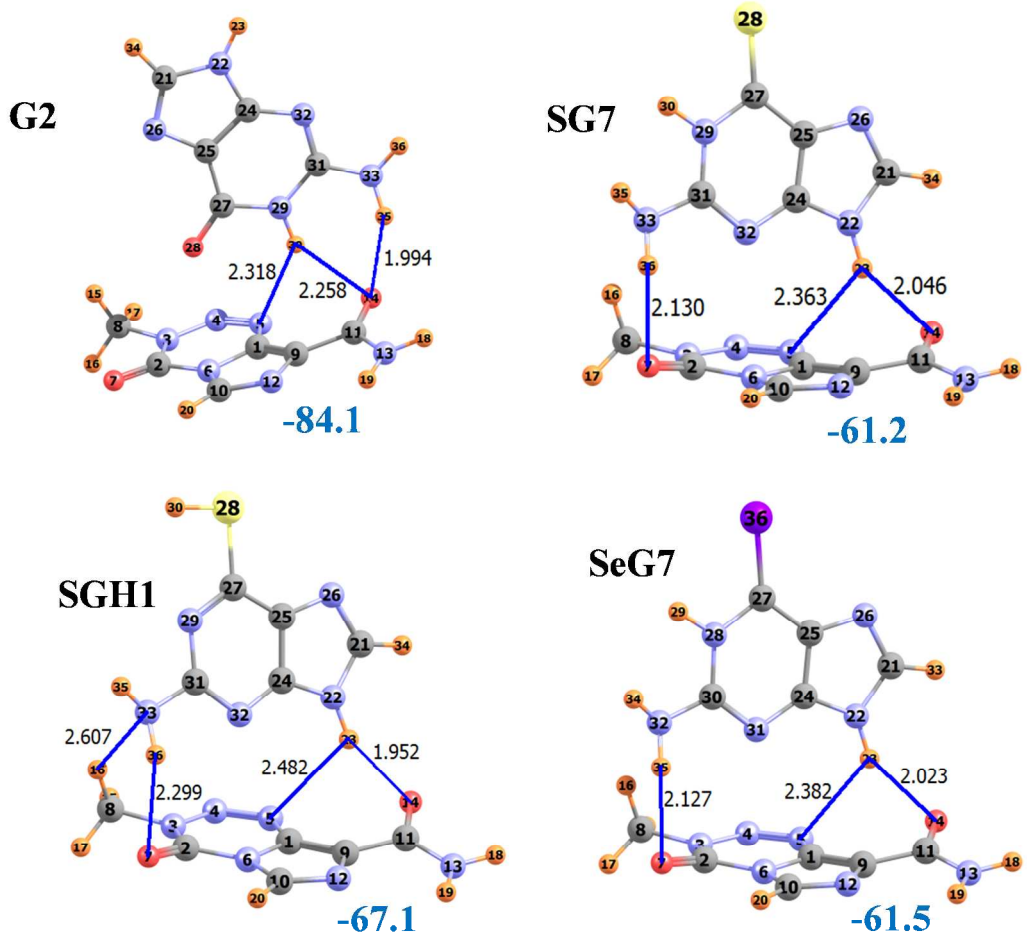

Fig 3. Geometries of the most stable perpendicular geometry of each guanine derivative with TMZ.

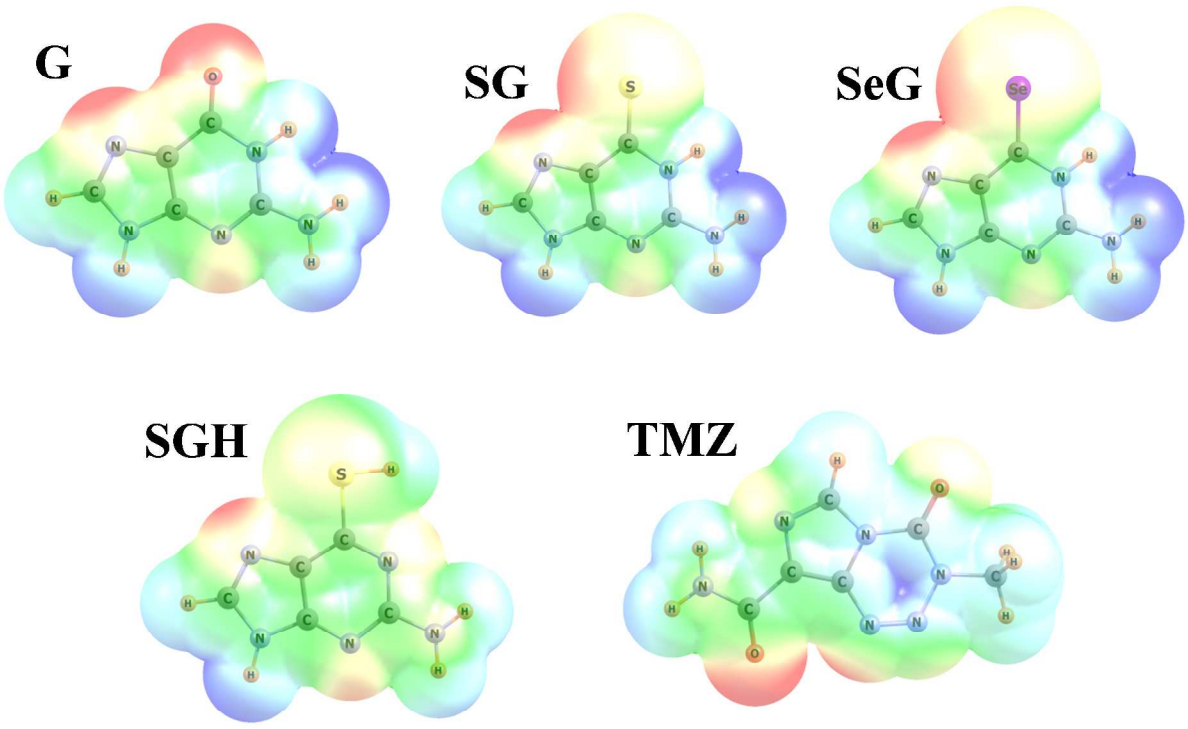

Fig 4. Molecular electrostatic potential surrounding each monomer on a surface representing 1.5 times the van der Waals radius of each atom. Blue color indicates a potential of +0.08 au and red corresponds to -0.08 au.

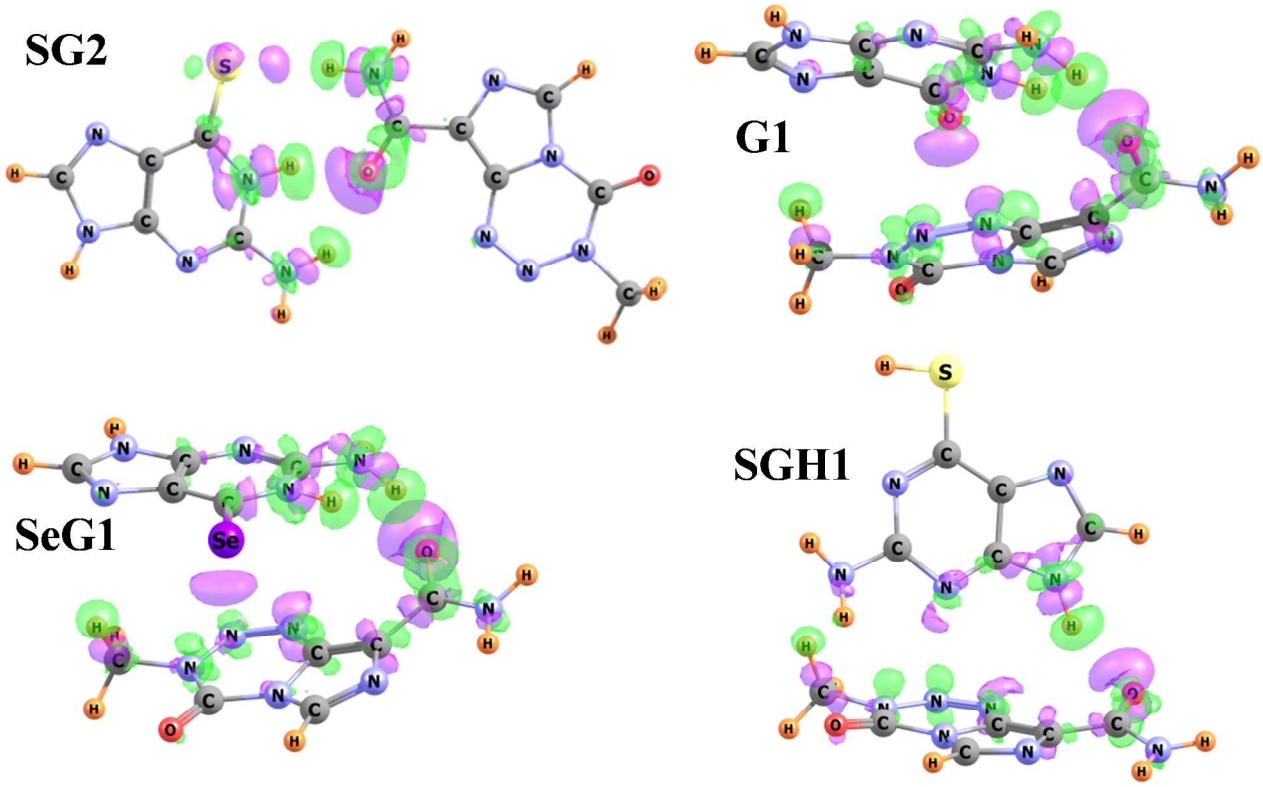

Fig 5. Electron density shifts occurring within dimers as a result of complexation. Purple and green regions respectively indicate gains and losses of density, at the ±0.002 au contour.

TOC graphic

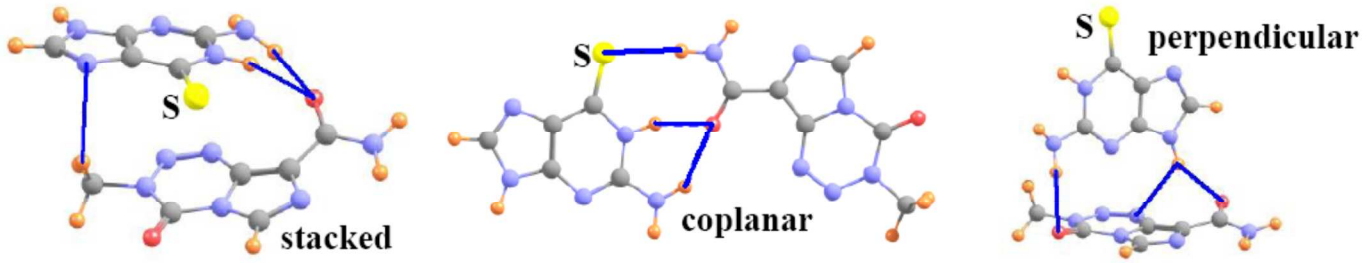

Replacement of O of guanosine by S or Se yields three different geometries of heterodimer complexes with temozolomide. This substitution has relatively little effect on preferred structures or energetics. Dispersion is most important for stacked arrangements, less so for perpendicular, and least for coplanar. Most minima contain H-bonds, even those that are dominated by π-π interactions.

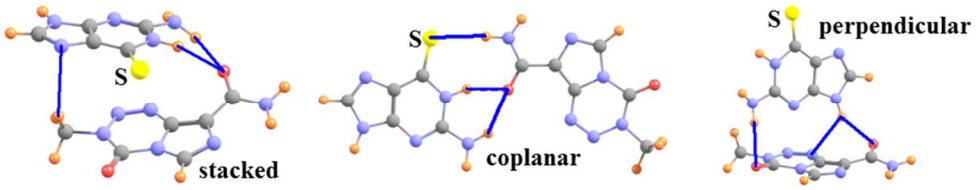

254x190mm (96 x 96 DPI)